Geochemistry
Geophysics
Geosystems

G³

AN ELECTRONIC JOURNAL OF THE EARTH SCIENCES

Published by AGU and the Geochemical Society

A model for the rheology of particle-bearing suspensions and partially molten rocks

Antonio Costa

Istituto Nazionale di Geofisica e Vulcanologia, I-80124 Naples, Italy

Centre for Environmental and Geophysical Flows, Department of Earth Sciences, University of Bristol, Bristol BS8 1RJ, UK (costa@ov.ingv.it)

Luca Caricchi

Department of Earth Sciences, ETH Zurich, CH-8092 Zurich, Switzerland

Now at Institut des Sciences de la Terre, Université d'Orleans, F-45071 Orleans CEDEX, France

Nickolai Bagdassarov

Institut für Geowissenschaften, Facheinheit Geophysik, Universität Frankfurt, D-60438 Frankfurt, Germany

[1] This contribution presents a semiempirical model describing the effective relative viscosity of crystal-bearing magmas as function of crystal fraction and strain rate. The model was applied to an extensive data set of magmatic suspensions and partially molten rocks providing a range of values for the fitting parameters that control the behavior of the relative viscosity curves as a function of the crystal fraction in an intermediate range of crystallinity (30–80 vol % crystals). The analysis of the results and of the materials used in the experiments allows for evaluating the physical meaning of the parameters of the proposed model. We show that the model, by varying the parameters within the ranges obtained during the fitting procedure, is able to describe satisfactory the effective relative viscosity as a function of crystal fraction and strain rate for suspensions having different geometrical characteristics of the suspended solid fraction.

1. Introduction

[2] A quantitative description of the rheology of solid-liquid suspensions is of a great interest in many application fields, encompassing extremes such as molding processes in industry or magma flow in geosciences. The knowledge of the rheology of magmas with large fraction of crystals is important

to define the dynamics of magma rise inside volcanic conduits, the extrusion of volcanic domes and more generally the dynamics of volcanic eruptions.

[3] Several studies on the rheological behavior of magmatic suspensions and partially molten systems were published in the last 30 years. The pioneering works of *Goetze* [1977] and *Arzi* [1978] dominated the view on the transition from a solid-state to a melt-dominated creep rheology, setting the threshold at a melt fraction about 0.25–0.30 (rheological critical melt percentage, RCMP). Successively, a number of experimental studies focused on the rheological behavior of melt-bearing materials. The rheology of partially molten rocks, with melt fractions lower than 0.12, was explored thoroughly by *Kohlstedt and Zimmerman* [1996]. The rheology of magma with solid fractions lower than 0.35–0.40 was investigated by *Pinkerton and Stevenson* [1992]. These observations highlighted the necessity to address the physical meaning of the critical melt fraction (transition from melt-dominated to solid-state creep rheology). Creep data on partially molten granites collected by *Rutter and Neumann* [1995] raised the question about the rapidity of the transition approaching the RCMP in a two phase system. *Vigneresse et al.* [1996] argued that the RCMP during crystallization differs from the RCMP during melting. The review of *Ji and Xia* [2002] explored a few different models of two-phase mixture rheology concluding that the relative viscosity of crystal supported systems and melt supported materials can be described using the *Reuss* [1929] and *Voigt* [1928] bounds. The exponential decrease of relative viscosity at the critical melt fraction was interpreted as a transition from iso-strain rate (solid-phase dominated; Voigt bound) to isostress (melt-phase dominated; Reuss bound) deformation conditions [e.g., *Takeda and Obata*, 2003]. *Petford* [2003] reviewed the existing literature and experimental data on rheology of magmatic suspensions and partially molten rocks. He pointed out the crucial role of the relationship between tortuosity and porosity for various packing densities in determining the position of the RCMP. *Rosenberg and Handy* [2005] identified two major rheological transitions occurring in partially molten rocks: the melt connectivity transition (MCT) occurring at melt fraction around 0.07, which induces a major decrease of the strength of the fully crystallized rock, and the second transition, defined as solid-liquid transition (SLT), occurring at melt fraction around 0.5 corresponding to the previously described RCMP.

[4] We present a semiempirical model able to describe the rheological effects of crystals from low to medium-high solid fractions, reproducing the transition from the regime where the strength is controlled by melt viscosity up to the beginning of the regime where strength is controlled by the solid framework, avoiding the singularity predicted by classical models at the maximum packing fraction [e.g., *Roscoe*, 1952; *Krieger and Dougherty*, 1959] Although we are aware that the relationship between stresses and strain rates for highly crystallized melts and partially molten rocks is very complex [see, e.g., *Renner et al.*, 2000; *Bercovici et al.*, 2001; *Rosenberg and Handy*, 2005] and can be nonunique, here our aim is to describe only an effective shear rheology of homogeneous systems of melts with crystals from low to medium-high solid fractions by means of a mathematical model, the adjustable parameters of which can be interpreted in terms of physical conditions of deformation experiments.

[5] The parameterization includes the strain rate–dependent rheology of partially crystallized materials. The analysis of the fitting results, taking into account the characteristics of the materials employed in the experiments and the application of some theoretical concepts on the rheology of two-phase mixtures, allow for assigning a physical meaning to the parameters of the proposed equations. Finally the effect of particle shapes and crystal size distribution on the variation of viscosity as function of crystal fraction and strain rate is also discussed.

2. Parameterization for Solid Fraction Dependence

[6] A quantitative description of the variations of viscosity as function of the solid fraction present several problems. The effective relative viscosity (ratio between the effective viscosity of the solid-liquid suspension and the viscosity of the liquid phase) needs to be introduced in many cases [see *Costa*, 2005]. Since viscosity controls magma transport, modeling of volcanic processes such as dome growth requires to estimate the viscosity dependence on crystal content, even in the limit of high solid fractions where few experimental observations are available [see, e.g., *Melnik and Sparks*, 1999, 2005; *Costa et al.*, 2007a, 2007b].

[7] A parameterization describing the relative viscosities of a melt-solid mixture, valid for relatively large solid fractions, was proposed by *Costa* [2005]. At low solid content the parameterization is approximately reduced to the well-established formulation of *Krieger and Dougherty* [1959]. However, for large particle volume fractions (φ), the parameterization suggested by *Costa* [2005] tends quickly to a constant value, because the nonlinear term in the error function ("erf") rapidly saturates as φ approaches unity. The *Costa* [2005] relationship for relative viscosity of concentrated suspensions was later improved and generalized by *Costa et al.* [2007a] (see also http://arxiv.org/pdf/physics/0512173). The parameterization used by *Costa et al.* [2007a, 2007b] is adopted also in the current study. The relationship between the relative viscosity and the particle volume fraction is described by:

$$\eta(\phi) = \frac{1 + \varphi^\delta}{[1 - F(\varphi, \varepsilon, \gamma)]^{B \cdot \phi_*}}, \tag{1}$$

where

$$F = (1 - \xi) \cdot \text{erf}\left[\frac{\sqrt{\pi}}{2 \cdot (1 - \xi)} \varphi \cdot (1 + \varphi^\gamma)\right] \text{ with } \varphi = \frac{\phi}{\phi_*}. \tag{2}$$

Here ϕ_* represents the critical solid fraction at the onset of the exponential increase of η; ξ ($\ll 1$), γ and δ are empirical parameters and B is the Einstein coefficient (i.e., the intrinsic viscosity) with a nominal value of 2.5. The parameter γ is a measure of the rapidity of relative viscosity increase with crystal fraction, as ϕ approaches ϕ_*. δ controls the increase of η at $\phi > \phi_*$. As demonstrated below, δ can be expressed in terms of γ as $\delta = A - \gamma$ where $A = 13$ is an empirical constant. For large δ, the second term in the numerator represents a negligible correction when $\phi < \phi_*$, while it becomes important when $\phi > \phi_*$. At $\phi = \phi_* \eta$ depends on ξ and ϕ_*, only:

$$\eta_* = \eta(\phi_*) = 2 \cdot \left[1 - (1 - \xi) \cdot \text{erf}\left(\frac{\sqrt{\pi}}{1 - \xi}\right)\right]^{-B \cdot \phi_*}. \tag{3}$$

Expanding F in equation (2) as a Taylor series [see *Costa*, 2005], it can be noticed that with decreasing ϕ, at $\phi < \phi_*$, equation (1) tends exactly to the *Krieger and Dougherty* [1959] relationship:

$$\eta = (1 - \phi/\phi_*)^{-B \cdot \phi_*}, \tag{4}$$

and when $\phi \to 0$, it recovers exactly to the Einstein equation:

$$\eta(\phi) = (1 + B \cdot \phi). \tag{5}$$

3. Model Applicability, Strain Rate Effects, Influence of Particle Shape, and Particle Size Distribution

[8] The rheology of a solid-fluid mixture is very complex and several simplifying assumptions need to be introduced. The full description of an isotropic linear medium requires the use of two viscosities, a bulk viscosity and a shear viscosity. Moreover, localized failure of partially molten rock does not permit a unique mapping between the space of stress and strain rate tensor [e.g., *Rutter and Neumann*, 1995].

[9] In order to simplify the problem we consider only homogeneous systems of melts with crystals from low to medium-high solid fractions. Results obtained above the percolation threshold of the solid matrix (the maximum solid fraction to obtain liquid interconnection) are considered merely as mathematical extrapolations. Moreover we describe the rheology of the homogenous systems simply by means of an effective shear viscosity, defined as the ratio between the maximum differential stress and the strain rate.

[10] Besides the increase in viscosity with crystal fraction, the rheology of highly concentrated solid-fluid mixture strongly depends on strain rate, crystal shapes and crystal size distribution. Concerning strain rate, *Caricchi et al.* [2007] experimentally showed that at relatively low strain rates ($10^{-6} - 10^{-5}$ s^{-1}) particle-silicate melt suspensions behave as a Newtonian liquid. Increasing strain rate ($\dot{\varepsilon}$), and consequently the applied stress, beyond these values induces a transition to non-Newtonian behavior (shear thinning) caused by a decrease of the degree of randomness of the particle distribution. At high enough strain rates ($\sim 10^{-3}$ s^{-1}), a maximum degree of ordering is reached and the effective viscosity is no longer strain rate–dependent. This high strain rate rheological behavior was observed in several particle-bearing suspensions and was defined as pseudo-Binghamian behavior [e.g., *van der Werff and de Kruif*, 1989; *Barnes*, 1999]. However, for the case of magmas, at large strain rates ($\dot{\varepsilon} > 10^{-3}$ s^{-1}), viscous heating can lead to an additional decrease of the melt viscosity [*Hess et al.*, 2008]. The proposed formulation considers the existence of a pseudo-Binghamian rheological field for $\dot{\varepsilon} > 10^{-3}$ s^{-1} and, as a conse-

quence, the presented model provides only an upper limit of effective relative viscosity at higher strain rates. The rheological transitions occurring with increasing strain rate from Newtonian to non-Newtonian and finally pseudo-Binghamian behavior, influence the parameters of equation (2). The parameters ϕ_*, ξ, γ and δ are nearly constant up to the transition to non-Newtonian behavior, they become, again, almost constant at a strain rate of about 10^{-3} s^{-1} where the mixture behaves as a pseudo-Bingham material. Parameters in equation (2) were empirically described by *Caricchi et al.* [2007] as a function of $\dot{\varepsilon}$ by:

$$\phi_* = \phi_t + \Delta\phi \tanh\left[b_\phi Log_{10}(\dot{\varepsilon}) + c_\phi\right],$$
$$\xi = \xi_t + \Delta\xi \tanh\left[b_\xi Log_{10}(\dot{\varepsilon}) + c_\xi\right],$$
$$\gamma = \gamma_t + \Delta\gamma \tanh\left[b_\gamma Log_{10}(\dot{\varepsilon}) + c_\gamma\right],$$
$$\delta = \delta_t - \Delta\delta \tanh\left[b_\delta Log_{10}(\dot{\varepsilon}) + c_\delta\right] \quad (6)$$

(for the numerical values of the empirical constants see equations (6)–(9) in the work by *Caricchi et al.* [2007]; in the work by *Caricchi et al.* [2007], $\alpha = 1 - \xi$). Results from *Caricchi et al.* [2007] show that ϕ_*, ξ and γ increase with increasing strain rate while δ decreases with increasing strain rate. Their experimental data also show that $c_\delta/b_\delta \approx c_\gamma/b_\gamma \approx c_\xi/b_\xi \approx c_\phi/b_\phi - 1$, indicating the occurrence of two characteristic strain rates $\dot{\varepsilon}_c$ and $\dot{\varepsilon}_d \approx 10 \cdot \dot{\varepsilon}_c$ that should be functions of the material properties. Moreover, their data suggest an approximately constant exponent for the dependence on $\dot{\varepsilon}$ in equations (6). After some analytical manipulations, equations (6) can be rewritten as:

$$\phi_* = \phi_m + \Delta\phi \frac{(\dot{\varepsilon}/\dot{\varepsilon}_c)^n - (\dot{\varepsilon}_c/\dot{\varepsilon})^n}{(\dot{\varepsilon}/\dot{\varepsilon}_c)^n + (\dot{\varepsilon}_c/\dot{\varepsilon})^n}$$
$$\xi = \xi_m + \Delta\xi \frac{(\dot{\varepsilon}/\dot{\varepsilon}_d)^n - (\dot{\varepsilon}_d/\dot{\varepsilon})^n}{(\dot{\varepsilon}/\dot{\varepsilon}_d)^n + (\dot{\varepsilon}_d/\dot{\varepsilon})^n}$$
$$\gamma = \gamma_m + \Delta\gamma \frac{(\dot{\varepsilon}/\dot{\varepsilon}_d)^n - (\dot{\varepsilon}_d/\dot{\varepsilon})^n}{(\dot{\varepsilon}/\dot{\varepsilon}_d)^n + (\dot{\varepsilon}_d/\dot{\varepsilon})^n}$$
$$\delta = \delta_m - \Delta\delta \frac{(\dot{\varepsilon}/\dot{\varepsilon}_d)^n - (\dot{\varepsilon}_d/\dot{\varepsilon})^n}{(\dot{\varepsilon}/\dot{\varepsilon}_d)^n + (\dot{\varepsilon}_d/\dot{\varepsilon})^n} \quad (7)$$

where $\phi_m = (\phi_\infty + \phi_0)/2$, $\Delta\phi = (\phi_\infty - \phi_0)/2$, $\xi_m = (\xi_\infty + \xi_0)/2$, $\Delta\xi = (\xi_\infty - \xi_0)/2$, $\gamma_m = (\gamma_\infty + \gamma_0)/2$, $\Delta\gamma = (\gamma_\infty - \gamma_0)/2$, and $\delta_m = (\delta_\infty + \delta_0)/2$, $\Delta\delta = (\delta_0 - \delta_\infty)/2$ with subscript ∞ indicating the values at very large $\dot{\varepsilon}$ and subscript 0 those at very low $\dot{\varepsilon}$. The best fit of the data of *Caricchi et al.* [2007] results $n \cong 0.33$, $Log_{10}(\dot{\varepsilon}_c) = -4.30$, $Log_{10}(\dot{\varepsilon}_d) = -3.37$, and the other parameter values as reported in the caption of Figure 1.

[11] Experimental data for polymer melts with different volume fraction of fibers suggest, in a limited range, a linear dependence of ϕ_* on the average aspect ratio [e.g., *Pabst et al.*, 2006] but further investigations are necessary. Experimental data for polymer melts with different volume fraction of fibers show a linear dependence of ϕ_* on the average aspect ratio [e.g., *Pabst et al.*, 2006]:

$$\phi_* = \phi_S - a_R(\overline{R} - 1), \quad (8)$$

where ϕ_s is the critical fraction for spherical particle, $\overline{R}$ is the average particle aspect ratio defined as ratio between the long and the short axes, and a_R is an empirical constant. The intrinsic viscosity B, here assumed constant for sake of simplicity, can also change with the aspect ratio [e.g., *Pabst et al.*, 2006]. However, the lack of experimental data at high solid fraction does not permit to constrain the values of the empirical parameters for which further experimental data and investigations are needed [e.g., *Mueller et al.*, 2008].

[12] Finally, experiments for bidispersed systems show that the smaller the particle diameter ratio the higher the critical solid fraction [e.g., *Chong et al.*, 1971]. The dependence of ϕ_* on the crystal size distribution can be given as [*Chong et al.*, 1971]:

$$\phi_* = \phi_{*md} \cdot \left(\frac{d}{D}\right)^{-0.1041}, \quad (9)$$

where ϕ_{*md} denotes the critical fraction for a monodispersed system, and d and D are the diameters of the smaller and bigger particles respectively.

4. Data Set for the Calibration of the Model

[13] *Bagdassarov and Dorfman* [1998] reported a noteworthy data set of effective relative viscosities of partially molten granite. Their study includes data from *Rutter and Neumann* [1995], *Auer et al.* [1981], *Rushmer* [1995], *Arzi* [1978], and *van der Molen and Paterson* [1979]. Effective relative viscosity was thereby considered as the ratio between effective viscosity of the partially molten rock and the viscosity of the melt phase.

[14] In order to calibrate the parameterization described by equation (2) we used all data mentioned above for large ϕ including data from *Lejeune and Richet* [1995], which measured relative viscosity of melt-particle suspensions up to solid fractions of 0.65 ($Mg_3Al_2Si_3O_{12}$), and results from *Caricchi et al.* [2007] for a water-bearing haplogranititc melt with suspended quartz particle fraction varying
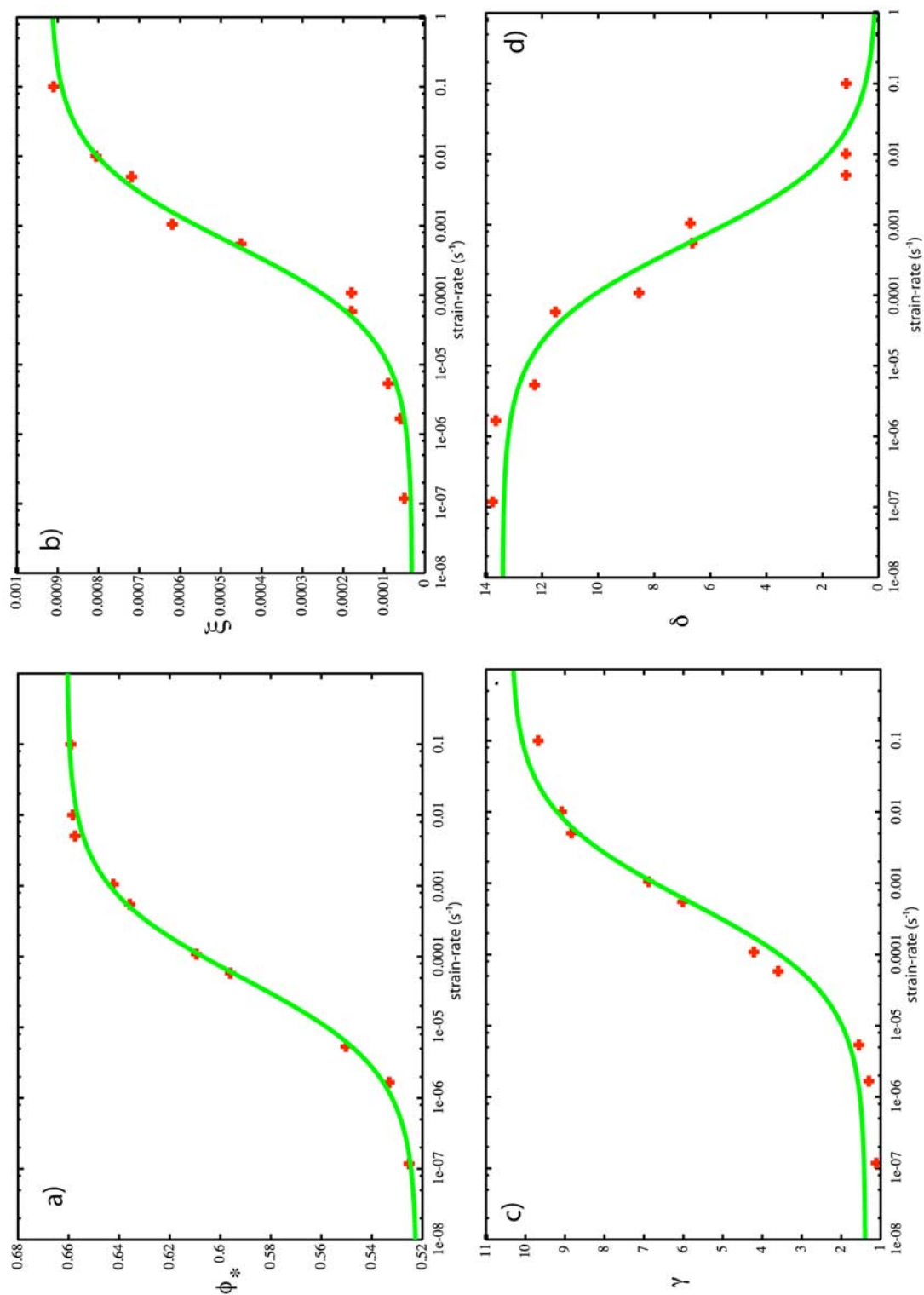
Figure 1. Strain rate dependence of parameters in equation (8) with $n \cong 0.33$, $\dot{\varepsilon}_c = 10^{-4.3}$ s^{-1}, and $\dot{\varepsilon}_d = 10^{-3.37}$ s^{-1}. (a) ϕ_* versus $\dot{\varepsilon}$ with $\phi_m = 0.591$ and $\Delta\phi_* = 0.069$, (b) ξ versus $\dot{\varepsilon}$ with $\xi_m = 4.63 \times 10^{-4}$, (c) γ versus $\dot{\varepsilon}$ with $\gamma_m = 5.76$ and $\Delta\gamma = 4.46$, and (d) δ versus $\dot{\varepsilon}$ with $\delta_m = 6.78$ and $\Delta\delta = 6.66$. The values reported in Figure 1 are from *Caricchi et al.* [2007].
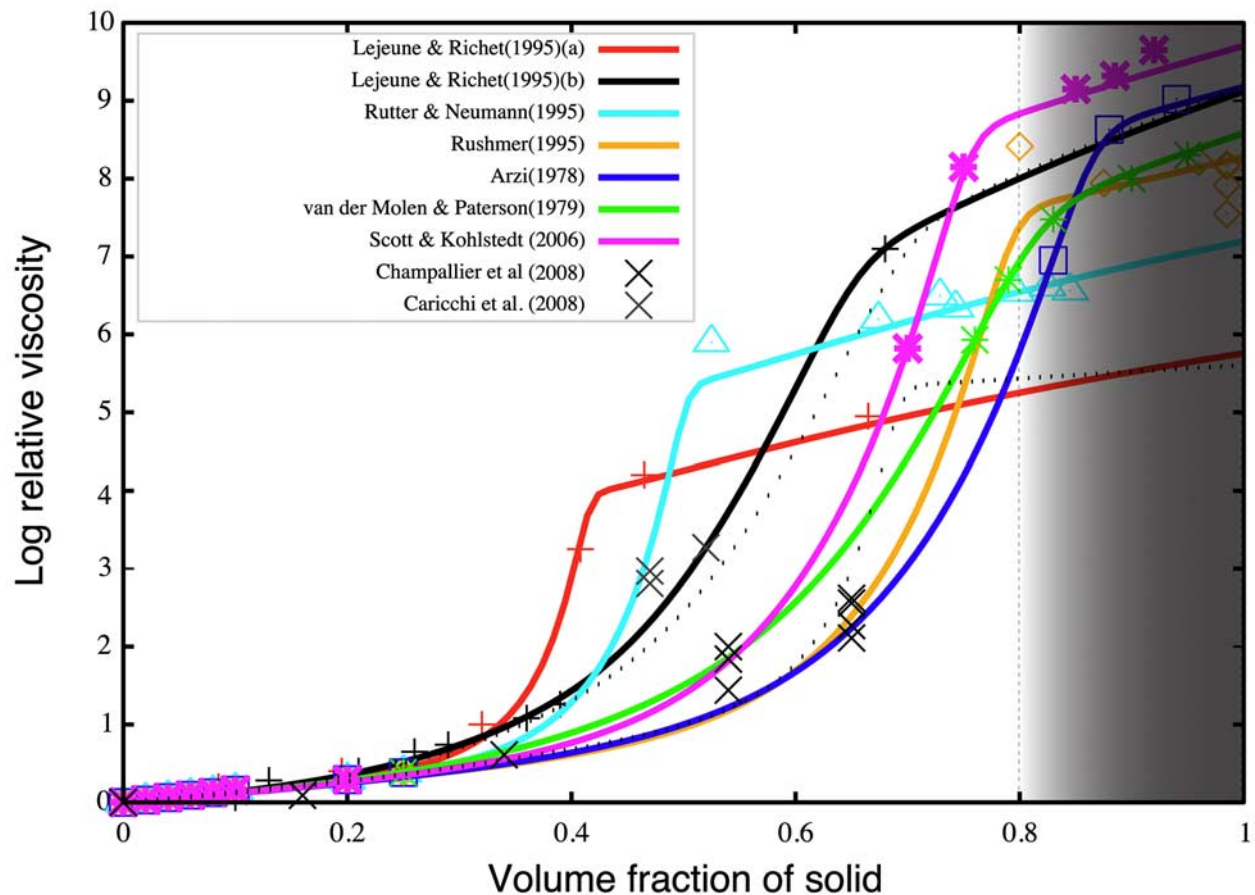
Figure 2. Variation of the logarithm of the effective relative viscosities with respect to the solid fraction for the data set reported in the inset. Dashed lines represent the bounding limits predicted by *Caricchi et al.* [2007]. $\delta = A - \gamma$ with $A = 13$. The gray shaded region denotes the region above the percolation threshold of the solid matrix (the maximum solid fraction to obtain liquid interconnection) where results need to be considered merely as mathematical extrapolations.

between 0.5 and 0.8. We also included data obtained from experiments with partially molten samples of olivine with MORB obtained by *Scott and Kohlstedt* [2006] and *Hirth and Kohlstedt* [1995] in the range of the strain rate from 10^{-6} to 10^{-4} s^{-1} for diffusion creep regime. Additional data for a system containing particles with aspect ratios of 1:2.5 (Li$_2$Si$_2$O$_5$ [*Lejeune and Richet*, 1995]) were also included. These data allow for investigating some particle shape effects on the fitting parameters. Data from *Champallier et al.* [2008] and *Caricchi et al.* [2008] were also considered in the data set for comparison. *Champallier et al.* [2008] conducted experiments on a system similar that investigated by *Caricchi et al.* [2007] in a strain rate range between $6 \cdot 10^{-4}$ and $2 \cdot 10^{-3}$ s^{-1}. *Caricchi et al.* [2008] investigated a natural material containing elongated plagioclase particles. The data at medium to high crystal fraction were combined with the values predicted by the Krieger-Dougherty relationship for $\phi < 0.1$ and data of *Thomas* [1965] for $\phi < 0.2$

to encompass the variation of the effective viscosity over the full range of solid fractions.

[15] The available information on applied strain rate and geometrical characteristics of the suspended particles were extracted from each set of data considered for the fitting procedure. However, there are some limitations for the data reported by *Arzi* [1978] and *Rutter and Neumann* [1995] that is worth stressing. *Arzi* [1978] reported values of relative viscosity of 10^8, 10^8 and 10^6 for samples having melt fractions of 0.06, 0.12, and 0.17 respectively. The experiments on the different specimens were performed at different temperatures and the relative viscosity was calculated using melt phase viscosity values reported by *Shaw* [1963]. Unfortunately, the temperature effect on the viscosity of the silicate melt was not carefully considered during the calculation of the relative viscosity. Using the *Hess and Dingwell* [1996] model, which is more general and also able to reproduce *Shaw*'s [1963] data, to

Table 1. Parameters Obtained by the Best Fit of Experimental Data

	Parameters[a]							
	1a	1b	2	3	4	5	6	7
ϕ_*	0.384	0.489	0.451	0.652	0.706	0.736	0.622	0.592 (0.52/0.66)
γ	7.701	1.440	6.220	1.911	5.142	3.679	3.429	7.462 (13.76/1.16)
$\xi \cdot 10^{-4}$	2.0	0.3	0.5	1.0	1.0	0.5	0.1	4.75 (0.32/9.18)
$\mathrm{Log}_{10}(\dot{\varepsilon})$ s^{-1}	−8/−6	−8/−6	−7/−4	−5	n.s.	n.s.	−6/−4	−6/−3

[a] Parameters 1a, *Lejeune and Richet* [1995] (for Li$_2$Si$_2$O$_5$); parameters 1b, *Lejeune and Richet* [1995] (for Mg$_3$Al$_2$Si$_3$O$_{12}$); parameters 2, *Rutter and Neumann* [1995]; parameters 3, *van der Molen and Paterson* [1979]; parameters 4, *Rushmer* [1995]; parameters 5, *Arzi* [1978]; parameters 6, *Scott and Kohlstedt* [2006] and *Hirth and Kohlstedt* [1995]; parameters 7, *Caricchi et al.* [2007]. For all calculations, $\delta = A - \gamma$ with $A = 13$. n.s. means "not specified" by the authors.

calculate the appropriate values of the melt viscosity at the experimental conditions investigated by *Arzi* [1978], the values of relative viscosity result 10^9, $10^{8.6}$ and $10^{6.9}$ for the sample with melt fraction 0.06, 0.12 and 0.17 respectively. Additionally, the applied stresses or strain rates are not reported for each experiment creating difficulties in evaluating the strain rate effect on the effective viscosity. The data of *Rutter and Neumann* [1995] present some uncertainties regarding the amount of melt present during the experiments. They used natural samples that are not in equilibrium at experimental conditions and, therefore, tend to react producing either melt or crystallizing mineral phases. Additionally, the authors report the difficulty to estimate the viscosity of the sample with the lowest ϕ (0.53−0.67) because the applied stress at flow was within the experimental error. Consequently, the reported value of viscosity for $\phi = 0.53$ is only an upper limit. As mentioned above, an additional aspect of the experiments performed by *Rutter and Neumann* [1995] that needs to be considered is the tendency, reported by the authors, of the samples to deform inhomogeneously. Brittle behavior and strain partitioning between the solid and liquid component of the deformed material is not accounted for by the model presented in this study.

5. Fitting Results

[16] In Figure 2 and Table 1 we present the results obtained by best fitting equation (2) with the data set described above. The results show that most of the available experimental data are within the range predicted by *Caricchi et al.* [2007] for different applied stress (or strain rate) conditions.

[17] One of the most important parameters determining the rheological behavior of a dense solid-liquid mixture is the critical solid fraction ϕ_*. This critical fraction delimits the transition from a system where the viscosity of the suspension is controlled by the viscosity of the liquid phase to a system where particle-particle interactions induce a strong increase of viscosity [*Caricchi et al.*, 2007]. The considered data set, summarized in Table 1, shows values of ϕ_* over a wide range of crystal fractions ranging from 0.38 to 0.74 with an average value around 0.57. The dependence of ϕ_* on the shear stress [*Caricchi et al.*, 2007; *Wildemuth and Williams*, 1984] can partly explain this variation. As mentioned above, particle dispersion and particle aspect ratio [*Chong et al.*, 1971; *Solomon and Boger*, 1998; *Yue et al.*, 1999; *Pabst et al.*, 2006] can additionally influencing ϕ_* (see equations (8) and (9)). More specifically elongated particles tend to decrease ϕ_* as confirmed by the data collected by *Lejeune and Richet* [1995] and *Caricchi et al.* [2008] (Figure 2).

6. Discussion

[18] The proposed model provides good fitting results of the experimental data (Figure 2) but for identifying the physical significance of the adjustable parameters it is worth highlighting their effects and interpreting the results on the basis of the theory of two-phase suspensions (see Appendix A).

[19] The bulk viscosity of a mixture of two phases is bounded by two curves defined as isostrain rate bound (called upper or Voigt bound) and the isostress bound (called lower or Reuss bound). A more accurate description of the variation of the effective viscosity against the crystal fraction can be obtained from Hashin-Shtrikman bounds. Upper and lower bounds for the relative viscosity can be calculated as (see Appendix A):

$$\eta_{HS}^+ = \frac{\mu_2}{\mu_1} - \frac{1 - \phi}{\dfrac{1}{\mu_2/\mu_1 - 1} + \dfrac{2}{5} \cdot C^+ \cdot \phi \cdot \dfrac{\mu_1}{\mu_2}}$$

$$\eta_{HS}^- = 1 + \frac{\phi}{\dfrac{1}{\mu_2/\mu_1 - 1} + \dfrac{2}{5} \cdot C^- \cdot (1 - \phi)} \tag{10}$$

where the symbol η denotes the ratio of the bulk viscosity to the soft phase viscosity, ϕ is the volume fraction of the more viscous phase, μ_1 denotes the soft phase viscosity, μ_2 represents the viscosity of the more viscous phase μ_{HS}^+ and μ_{HS}^- denote the upper and the lower bound for shear viscosity of the two phase system, and $C^\pm$ is a constant (for a melt and solid mixture $C^+ = 1$ and $C^- = 9/7$).

[20] The viscosity for the case of solid-phase supported flow is computed as the upper Hashin-Shtrikman boundary (or isostrain model); the flow, in this case, is controlled by the strain rate of the solid matrix. Conversely at high melt fraction the pressure or the shear stress is equal for both solid and melt phase and the flow is controlled by the soft phase. In this condition the viscosity corresponds to the lower Hashin-Shtrikman bound (or isostress case). Therefore, we know the two limits to which relative viscosity tends as $\phi \to 0$ and $\phi \to 1$ respectively. The variations of relative viscosity in an intermediate range of solid fractions are related to the geometrical characteristics and size distribution of the suspended particles, and to the applied strain rate conditions. More precisely the applied strain rates influence the degree of randomness of the suspended particles, which, in turn, results in different trends of relative viscosity variation as function of the particle fraction.

[21] Figure 3 summarizes the effects of the parameters used in equations (1) and (2) on the variations of viscosity with respect to crystal fraction. The critical solid fraction ϕ_* defines the limit of the regime where the viscosity is mainly controlled by the melt phase from the regime where interactions among particles have a pivotal role. The lowest values of ϕ_* are characteristic for suspensions containing elongated particles (Figure 2). Increase of particle sphericity, strain rates and poly dispersion (wider distribution of particle sizes) results in an increase of ϕ_*, which produces trends similar to those shown in Figure 3c.

[22] As mentioned above, δ controls the maximum value of effective relative viscosity as ϕ tends to 1 (Figure 3a). Consequently, large values of δ are expected for suspensions containing particles with high resistance to deformation (i.e., high viscosity). The parameter γ controls the sharpness of the viscosity increase around the critical particle fraction (Figure 3b). The increase of the viscosity at the critical solid fraction is related to a strong increase of the tortuosity of the melt flow patterns [*Gibilaro*, 2001] due to the achievement of a continuous crystal framework. Suspensions containing randomly ori-

ented particles are characterized by higher tortuosity of the melt flow patterns and consequently by relatively high values of γ. This observation is confirmed by the *Caricchi et al.* [2007] data in which the ordering of the particles, caused by higher applied strain rates, induces a strong decrease of γ (from $\sim$14 at 10^{-6} s^{-1} to $\sim$1 at 10^{-3} s^{-1}).

[23] As previously reported, experimental data show an empirical relationship between δ and γ ($\delta = A - \gamma$ with $A = 13$), allowing for reducing the number of free parameters. Moreover, this implies that the steeper the transition around the critical fraction ϕ_* (controlled by γ) the smoother the increase of viscosity at larger solid fractions.

[24] Concerning ξ, equation (3) shows that, for a given ϕ_*, it determines the value of the characteristic viscosity $\eta_* = \eta(\phi_*)$. Like δ, also ξ plays an important role in determining the relative viscosity at very high solid fraction. In fact, from equations (1) and (2) we can show that in the limit $\phi \to 1$ we have:

$$\eta \sim \frac{1}{\xi^{B\phi_*}}\left(1 + \frac{\phi^\delta}{\phi_*^\delta}\right) \approx \frac{1}{\xi^{B\phi_*}}\left(1 + \phi_*^{-\delta}\right). \qquad (11)$$

[25] These indications provide some constraints on the physical significance of the variations of the adjustable parameters. The additional effect due to strain rate are illustrated in Figure 2 and mathematically formulated in equation (8).

[26] The relationship between effective yield stress and melt fraction (see Appendix A) is valid up to the percolation limit of the solid matrix, ϕ_C, i.e., the maximum solid fraction to obtain liquid interconnection [*Zhou et al.*, 1995]. For higher ϕ, particles start to deform substantially under the application of stress thereby inducing a rheological change from two-phase suspension to solid rock deformation.

[27] Additional experimental data exploring the effects of crystal size distributions, crystal shapes, and viscous heating at high strain rates are required to define accurately the range of variation of the fitting parameters as a function of the geometrical properties of the suspended particles.

7. Conclusions

[28] The effects of crystal fraction and strain rate on the rheology of partially crystallized magmas was presented and discussed. The proposed parameterization allows for describing variations of 6−9 orders of magnitude of the relative viscosity due
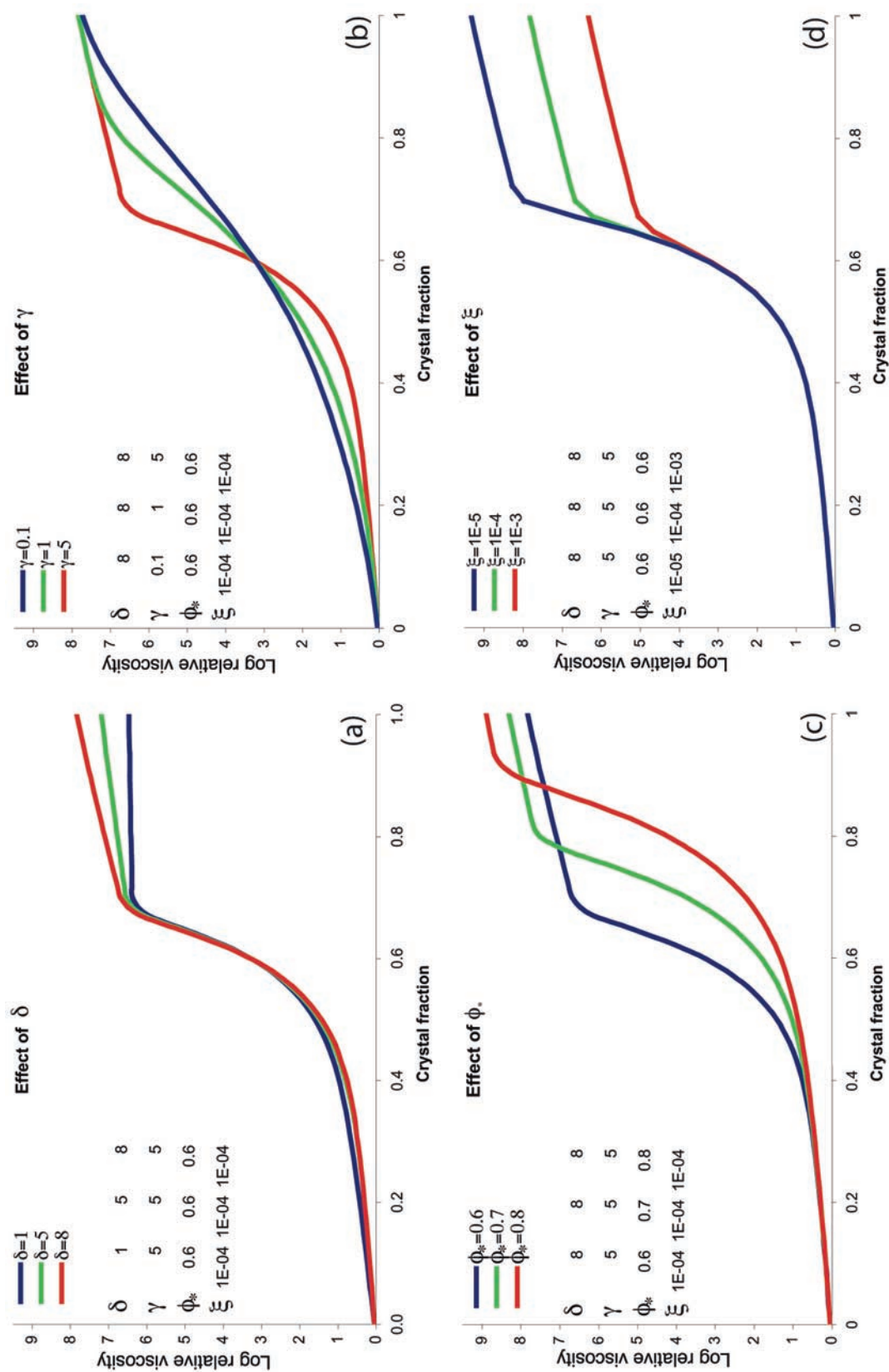
Figure 3. Effect of the variation of single parameters on the effective relative viscosities with respect to the solid fraction for the specific values reported in the inset.

to the presence of crystals and up to 3 orders of magnitude due to shear thinning for a large experimental data set. The uncertainties in the relative proportions of melt and crystals and the lack of information on important experimental conditions (e.g., applied strain rate), result in 1–2 orders of magnitude uncertainty for effective relative viscosity at high crystal fractions. The influence of the parameters on the relative viscosity curve with respect to the crystal fraction is presented and their variations associated with changes of the geometries of the suspended particles and different applied stress (or strain rate).

Appendix A

[29] In order to identify and interpret the physical significance of the adjustable parameters of the semiempirical model presented in this paper and some limitations of the model itself, here we briefly describe some concepts of the theory of two-phase suspensions.

[30] Lets revisit the rheology of a suspension consisting of two phases. The rheology of a mixture of two phases in general can be bounded by two curves which are called isostress model (the Reuss bound) and isostrain rate model (the Voigt bound), for details see *Ji and Xia* [2002] and *Takeda and Obata* [2003]. These two viscosity bounds are valid for pure shear deformation. In the case of a uniaxial deformation the situation is more complicated, instead of a shear stress, the sample is sheared because of the normal stress difference. Until the total deformation remains small, i.e., up to the point when the sample becomes anisotropic (i.e., no melt segregation, uniform compaction regime), the measured viscosity is a combination of the volume (bulk) and shear viscosity of sample, and the interpretation of the experimental results is based on the assumptions about bulk and shear viscosities of two phases [*McKenzie*, 1984; *Ricard et al.*, 2001]. Splitting bulk and shear viscosities from the results of rock deformation experiments is not very common but it is still adequate if we consider crystal concentrations in the medium to medium-high solid fraction range.

[31] Let us consider two more robust and general bounds of the effective relative viscosity of a two phase mixture, that can be derived from Hashin-Shtrickman bounds (HS$^\pm$). If we assume the analogy between elastic and viscous cases of deformation, the Hashin-Shtrickman bounds for the shear viscosity can be obtained from the expression for the shear modulus of a two component mixture [*Mavko et al.*, 1998]:

$$\mu^{HS\pm} = \mu_1 + \frac{\phi}{(\mu_2 - \mu_1)^{-1} + \frac{2}{5} \cdot \frac{(1 - \phi)}{\mu_1} \cdot C^\pm}, \qquad (A1)$$

where μ is the shear viscosity of the two phases, ϕ is the volume fraction of the more viscous phase, $C^\pm$ is a constant. Upper and lower boundaries are interchanged swapping the indexes of phase 1 and 2. For the mixture of melt and solid phase $C^+ = 1$ and $C^- = 9/7$, respectively. In the elastic case, the constant $C^\pm$ is the ratio $(K + 2\mu)/(K + 4/3\mu)$, where K and μ are the bulk and shear modulus. In the viscous case instead of K one needs to insert a volume viscosity, which, for the solid phase, is infinity and for liquid phase is about the value of the shear viscosity. The sample flow supported by solid phase is the case of the upper Hashin-Shtrickman boundary or isostrain model. The total sample flow in this case is controlled by the strain rate of a solid matrix. At high melt fractions the flow is supported by the soft phase, the pressure or the shear stress is equal in two phases. Thus, this situation corresponds to a lower Hashin-Strickman boundary or isostress case.

[32] Basically, the behavior of a flow with or without drainage can be understood as a smooth transition from one Hashin-Shtrickman boundary to another (see Figure A1). With respect to the Voigt and Reuss averaging the Hashin-Strickman bounds exclude anisotropic microstructures in two phase mixtures, but essentially they correspond to two limiting situations: the isostress (μ^{HS-}) and isostrain rate (μ^{HS+}) rheologies of a two component mixture.

[33] Concerning the dependence on the strain rate, the relative viscosity of two phase mixture can be formally written in a form of Cross equation [e.g., *Barnes*, 1999]:

$$\mu = \mu_\infty + \frac{(\mu_0 - \mu_\infty)}{1 + (\tau \cdot \dot\varepsilon)^m}, \qquad (A2)$$

where μ_∞ und μ_0 are the viscosities at very high and very slow strain rates, τ is the characteristic time of viscous stress relaxation and $\dot\varepsilon$ is the strain rate. Here again, τ represents an effective time scale, which separates two extreme rheological cases: with and without building of the pressure difference between two phases. In equation (A2), for Newtonian viscosity $m = 2$, for non-Newtonian behavior $1 < m < 2$. The relaxation time spectrum is
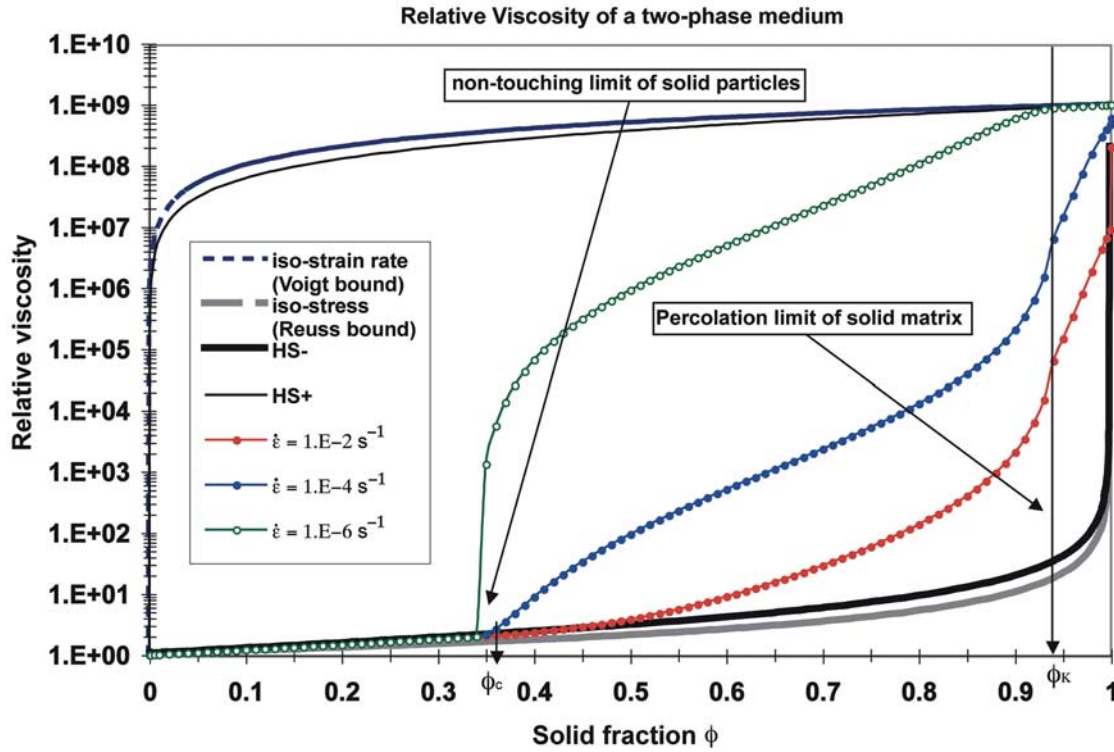
Figure A1. Examples of relative viscosities of a two phase mixture and bounds calculated using equations (A1), (A3), and (A4) using different parameters. The contrast of viscosities between the hard and the soft phase is assumed to be 10^9; the strength of the solid phase is arbitrarily taken to be 10^8 Pa. In equation (A3) we set $m = 2$, and the stress σ was replaced by the product of a melt shear viscosity times the strain rate values indicated in the inset; in equation (A4) we set $C = 5 \cdot 10^4$ Pa, $\varphi_K = 0.35$, $\varphi_c = 0.95$, $n = 1$, and $k = 1$.

difficult to infer for mixtures, in the work by *Renner et al.* [2000], τ has been related to the pore pressure relaxation time. A more practical expression which includes shear stress σ and pseudo−yield stress σ_y is the Ellis empirical equation [*Barnes*, 1999]:

$$\mu = \mu_\infty + \frac{(\mu_0 - \mu_\infty)}{1 + (\sigma/\sigma_Y)^m}. \qquad (A3)$$

In the case of a two phase mixture we may associate the low-stress rheology with the situation when the liquid phase surrounds the solid phase $\mu_\infty = \mu^{HS-}$ (at $\phi \ll 1$). The high-stress rheology corresponds to the rheology in the isostrain rate case or the upper Hashin-Strickman boundary $\mu_0 = \mu^{HS+}$. The scale of stress σ in equation (A3) can be taken formally as a product of melt viscosity and strain rate.

[34] A mixture of a solid and a liquid phase is characterized by two concentration limits of the solid phase between which the yield stress σ_y varies as a smooth function of ϕ. There are a nontouching limit of concentration, ϕ_K, and a percolation threshold of the solid matrix, ϕ_c. According to *Barnes* [1999], this means that, if the solid fraction ϕ is

between these two limiting cases, the mixture has two viscosities: at high stresses the mixture will flow with a smaller viscosity, whereas at low stresses the viscosity will become higher and the flow is creeping. The variation of the yield stress σ_y as a function of ϕ between these two concentrations $\phi_K < \phi < \phi_c$ is given by *Barnes* [1999]:

$$\sigma_Y = C \cdot \frac{(\phi - \phi_K)^n}{(\phi_c - \phi)^k}, \qquad (A4)$$

where C, n and k are empirical constants describing how fast the yield stress σ_y varies between the two limiting concentrations. Above the percolation threshold, $\phi > \phi_c$, the yield stress σ_y is a smooth monotonic function of melt concentration up to the yield strength of the solid phase with closed porosity, $\phi = 1$. The effective shear stress appears to be a monotonously increasing function from the solid phase fraction ϕ_K up to ϕ_c. Then, σ_y increases stepwise with the decrease of porosity reaching the value of the yield stress of a solid matrix. The critical porosity of the solid matrix ϕ_c is associated with the rupture of a critical cluster according to

the percolation theory [*Guéguen and Palcialuskas*, 1994].

[35] The introduction of an "effective" or a pseudo-yield stress σ_Y can implicitly incorporate a drainage effect of melt in the matrix and interaction effects between melt and solid phase. For the relaxation of the melt overpressure a diffusion type of equation can been used, with a relaxation time inversely proportional to the permeability of the solid matrix. Approaching the percolation threshold, the relaxation time tends to a power law on porosity [*Renner et al.*, 2000]. The problem of the description of this low melt concentration regime is out of the scope of this paper.

[36] The transition from high-viscosity to lower-viscosity regime in creep experiments with partially molten samples of olivine with MORB was described by *Scott and Kohlstedt* [2006] in the range of the strain rate from 10^{-6} to 10^{-4} s^{-1}. The underlined mechanism has been attributed to the transitional nature of the creep process, from diffusion creep at low strain rates to grain boundary sliding at high strain rates. The variation of the grain size in samples influences the proportionality constant in equation (A4), $C \sim d^{-2}$ [*Barnes*, 1999]. In smaller grain size mixture the relative viscosity tends to the upper Hashin-Shtrickman boundary μ^{HS+} and the rheologically critical melt threshold shifts to larger melt fractions.

[37] As an example, in Figure A1 we show few case of relative viscosities of a two phase mixture and corresponding bounds calculated using equations (A1), (A3), and (A4) using the parameter values reported in the caption.

[38] Obviously this kind of description of a two phase rheology is a simplified idealization. However, the shape of the curves plotted in Figure A1 obtained from equations (A1), (A3) and (A4) mimics the trend of the experimental results and it is qualitatively similar to the behavior of the model discussed in this paper.

Acknowledgment

References

Arzi, A. (1978), Critical phenomena in the rheology of partially melted rocks, *Tectonophysics*, *44*, 173–184, doi:10.1016/0040-1951(78)90069-0.

Auer, F., H. Berkhemer, and G. Oehlschlegel (1981), Steady state creep of fine grain granite at partial melting, *J. Geophys.*, *49*, 89–92.

Bagdassarov, N., and A. Dorfman (1998), Granite rheology: Magma flow and melt migration, *J. Geol. Soc.*, *155*, 863–872, doi:10.1144/gsjgs.155.5.0863.

Barnes, H. (1999), The yield stress–a review or '$\pi\alpha\nu\tau\alpha\ \rho\epsilon\iota$'–everything flows?, *J. Non-Newtonian Fluid Mech.*, *81*, 133–178, doi:10.1016/S0377-0257(98)00094-9.

Bercovici, D., Y. Ricard, and G. Schubert (2001), A two-phase model of compaction and damage: 1. General theory, *J. Geophys. Res.*, *106*(B5), 8887–8906, doi:10.1029/2000JB900430.

Caricchi, L., L. Burlini, P. Ulmer, T. Gerya, M. Vassalli, and P. Papale (2007), Non-Newtonian rheology of crystal-bearing magmas and implications for magma ascent dynamics, *Earth Planet. Sci. Lett.*, *264*, 402–419, doi:10.1016/j.epsl.2007.09.032.

Caricchi, L., D. Giordano, L. Burlini, P. Ulmer, and C. Romano (2008), Rheological properties of magma from the 1538 eruption of Monte Nuovo (Phlegrean Fields, Italy): An experimental study, *Chem. Geol.*, *256*, 158–171, doi:10.1016/j.chemgeo.2008.06.035.

Champallier, R., M. Bystricky, and L. Arbaret (2008), Experimental investigation of magma rheology at 300 MPa: From pure hydrous melt to 76 vol. % of crystals, *Earth Planet. Sci. Lett.*, *267*, 571–583, doi:10.1016/j.epsl.2007.11.065.

Chong, J., E. Christiansen, and A. Baer (1971), Rheology of concentrated suspension, *J. Appl. Polym. Sci.*, *15*, 2007–2021, doi:10.1002/app.1971.070150818.

Costa, A. (2005), Viscosity of high crystal content melts: Dependence on solid fraction, *Geophys. Res. Lett.*, *32*, L22308, doi:10.1029/2005GL024303.

Costa, A., O. Melnik, and R. Sparks (2007a), Controls of conduit geometry and wall rock elasticity on lava dome eruptions, *Earth Planet. Sci. Lett.*, *260*, 137–151, doi:10.1016/j.epsl.2007.05.024.

Costa, A., O. Melnik, R. Sparks, and B. Voight (2007b), Control of magma flow in dykes on cyclic lava dome extrusion, *Geophys. Res. Lett.*, *34*, L02303, doi:10.1029/2006GL027466.

Gibilaro, L. G. (2001), *Fluidization-Dynamics*, 256 pp., Butterworth-Heinemann, Oxford, U. K.

Goetze, C. (1977), A brief summary of our present day understanding of the effect of volatiles and partial melt on the mechanical properties of the upper mantle, in *High-Pressure Research: Applications in Geophysics*, edited by M. H. Manghnani and S. Akimoto, pp. 3–23, Academic, New York.

Guéguen, Y., and V. Palcialuskas (1994), *Introduction to the Physics of Rocks*, 294 pp., Princeton Univ. Press, Princeton, N. J.

Hess, K. U., and D. B. Dingwell (1996), Viscosities of hydrous leucogranite melts: A non-Arrhenian model, *Am. Mineral.*, *81*, 1297–1300.

Hess, K., B. Cordonnier, Y. Lavallée, and D. B. Dingwell (2008), Viscous heating in rhyolite: An in situ experimental, *Earth Planet. Sci. Lett.*, *275*, 121–126, doi:10.1016/j.epsl.2008.08.014.

Hirth, G., and D. L. Kohlstedt (1995), Experimental constraints on the dynamics of the partially molten upper mantle: Deformation in the diffusion creep regime, *J. Geophys. Res.*, *100*, 1981–2001, doi:10.1029/94JB02128.

Ji, S., and B. Xia (2002), *Rheology of Polyphase Earth Materials*, 300 pp., Polytech. Int. Press, Québec, Que., Canada.

Kohlstedt, D. L., and M. E. Zimmerman (1996), Rheology of partially molten mantle rocks, *Annu. Rev. Earth Planet. Sci.*, *24*, 41–62, doi:10.1146/annurev.earth.24.1.41.

Krieger, I., and T. Dougherty (1959), A mechanism for non-Newtonian flow in suspension of rigid spheres, *Trans. Soc. Rheol.*, *3*, 137–152, doi:10.1122/1.548848.

Lejeune, A., and P. Richet (1995), Rheology of crystal-bearing silicate melts: An experimental study at high viscosity, *J. Geophys. Res.*, *100*, 4215–4229, doi:10.1029/94JB02985.

Mavko, G., T. Mukerji, and J. Dvokin (1998), *The Rock Physics Handbook, Tools for Seismic Analysis in Porous Media*, 329 pp., Cambridge Univ. Press, Cambridge, U. K.

McKenzie, D. (1984), The generation and compaction of partially molten rocks, *J. Petrol.*, *25*, 713–765.

Melnik, O., and R. S. J. Sparks (1999), Nonlinear dynamics of lava dome extrusion, *Nature*, *402*, 37–41, doi:10.1038/46950.

Melnik, O., and R. S. J. Sparks (2005), Controls on conduit magma flow dynamics during lava dome building eruptions, *J. Geophys. Res.*, *110*, B02209, doi:10.1029/2004JB003183.

Mueller, S., H. Mader, and E. Llewellin (2008), The influence of crystal shape on magma rheology, paper presented at IAVCEI General Assembly, Int. Assoc. of Volcanol. and Chem. of the Earth's Inter., Reykjavík, Iceland, 18–25 Aug.

Pabst, W., E. Gregorova, and C. Berthold (2006), Particle shape and suspension rheology of short-fiber systems, *J. Eur. Ceram. Soc.*, *26*, 149–160, doi:10.1016/j.jeurceramsoc.2004.10.016.

Petford, N. (2003), Rheology of granitic magmas during ascent and emplacement, *Annu. Rev. Earth Planet. Sci.*, *31*, 399–427, doi:10.1146/annurev.earth.31.100901.141352.

Pinkerton, H., and R. Stevenson (1992), Methods of determining the rheological properties of magmas at sub-solidus temperatures, *J. Volcanol. Geotherm. Res.*, *53*, 47–66, doi:10.1016/0377-0273(92)90073-M.

Renner, J., B. Evans, and G. Hirth (2000), On the rheologically critical melt fraction, *Earth Planet. Sci. Lett.*, *181*, 585–594, doi:10.1016/S0012-821X(00)00222-3.

Reuss, A. (1929), Berechnung des Fliessgrenze von Mischkristallen auf Grund der Plastizitätsbedingung für Einkristalle, *Z. Angew. Math. Phys.*, *9*, 49–58.

Ricard, Y., D. Bercovici, and G. Schubert (2001), A two-phase model for compaction and damage: 2. Application to compaction, deformation, and the role of interface tension, *J. Geophys. Res.*, *106*, 8907–8924, doi:10.1029/2000JB900431.

Roscoe, R. (1952), The viscosity of suspensions of rigid spheres, *Br. J. Appl. Phys.*, *3*, 267–269.

Rosenberg, C., and M. Handy (2005), Experimental deformation of partially melted granite revisited: Implications for the continental crust, *J. Metamorph. Geol.*, *23*, 19–28, doi:10.1111/j.1525-1314.2005.00555.x.

Rushmer, T. (1995), An experimental deformation study of partially molten amphibolite: Application to low-melt frac-tion segregation, *J. Geophys. Res.*, *100*, 15,681–15,695, doi:10.1029/95JB00077.

Rutter, E., and D. Neumann (1995), Experimental deformation of partially molten Westerly granite under fluid-absent conditions, with implications for the extraction of granitic magmas, *J. Geophys. Res.*, *100*, 15,697–15,715, doi:10.1029/94JB03388.

Scott, T., and D. L. Kohlstedt (2006), The effect of large melt fraction on the deformation behaviour of peridotite, *Earth Planet. Sci. Lett.*, *246*, 177–187, doi:10.1016/j.epsl.2006.04.027.

Shaw, H. (1963), Obsidian-HO viscosities at 1000 and 2000 bars in the temperature range 700°C to 900°C, *J. Geophys. Res.*, *68*, 6337–6343.

Solomon, M., and D. Boger (1998), The rheology of aqueous dispersions of spindle-type colloidal hematite rods, *J. Rheol.*, *42*, 929–949, doi:10.1122/1.550961.

Takeda, Y.-T., and M. Obata (2003), Some comments on the rheologically critical melt percentage, *J. Struct. Geol.*, *25*, 813–818, doi:10.1016/S0191-8141(02)00080-9.

Thomas, D. (1965), Transport characteristics of suspensions: VIII. A note on the viscosity of Newtonian suspensions of uniform spherical particles, *J. Colloid Sci.*, *20*, 267–277, doi:10.1016/0095-8522(65)90016-4.

van der Molen, I., and M. Paterson (1979), Experimental deformation of partially melted granite, *Contrib. Mineral. Petrol.*, *70*, 299–318, doi:10.1007/BF00375359.

van der Werff, J. C., and C. G. de Kruif (1989), Hard-sphere colloidal dispersions: The scaling of rheological properties with particle size, volume fraction, and shear Rate, *J. Rheol.*, *33*, 421–454, doi:10.1122/1.550062.

Vigneresse, J. C., P. Barbey, and M. Cuney (1996), Rheological transitions during partial melting and crystallization with application to felsic magma, *J. Petrol.*, *37*(6), 1579–1600, doi:10.1093/petrology/37.6.1579.

Voigt, W. (1928), *Lehrbuch der Kristallphysik*, Teubner, Leipzig, Germany.

Wildemuth, C., and M. Williams (1984), Viscosity of suspensions modeled with a shear-dependent maximum packing fraction, *Rheol. Acta*, *23*, 627–635, doi:10.1007/BF01438803.

Yue, Y., C. Moisescu, G. Carl, and C. Russel (1999), The influence of suspended iso-and anisometric crystals on the flow behavior of fluoroapatite glass melts during extrusion, *Phys. Chem. Glasses*, *40*, 243–247.

Zhou, J. Z. Q., T. Fang, G. Luo, and P. H. T. Ulherr (1995), Yield stress and maximum packing fraction of concentrated suspensions, *Rheol. Acta*, *34*, 544–561, doi:10.1007/BF00712315.